

Regio-Specific Selenium Substitution in Non-Fullerene Acceptors for Efficient Organic Solar Cells

Francis Lin,^{†,‡} Lijian Zuo,[‡] Ke Gao,[‡] Ming Zhang,[§] Sae Byeok Jo,[‡] Feng Liu,^{*,§} and Alex K-Y. Jen^{*,†,‡,⊥}

[†]Department of Chemistry, University of Washington, Seattle, WA 98195-2120, USA

[‡]Department of Materials Science and Engineering, University of Washington, Seattle, WA 98195-2120, USA

[§]Department of Physics and Astronomy, Shanghai Jiaotong University, Shanghai 200240, China

[⊥]Department of Chemistry and Department of Physics & Materials Science, City University of Hong Kong, Kowloon, Hong Kong

* E-mail: fengliu82@sjtu.edu.cn

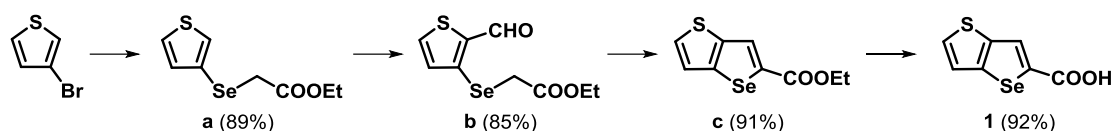
* E-mail: alexjen@cityu.edu.hk

Supporting Information

Table of Contents

Synthesis of Compound 1.....	S2
UV-Vis Measurement.....	S4
Electrochemical Measurement.....	S5
Photovoltaic Device Characteristics.....	S6
SCLC Characteristics.....	S7
GIWAXS Characteristics.....	S8
Reference.....	S10
¹ H and ¹³ C NMR Spectra.....	S11

Synthesis of Compound 1



Synthesis of ethyl 2-(thiophen-3-ylselanyl)acetate (a). To a stirred solution of 3-bromothiophene (78.3 g, 480 mmol) in dry diethyl ether (500 mL) was dropwise added *n*-BuLi (2.5 M in hexanes, 200 mL) at -78 °C over 30 minutes. The mixture was kept at -78 °C for one hour, after which selenium powder (40.9 g, 518 mmol) was added in small portions. The mixture was kept at -78 °C for one more hour, and was slowly warmed to -40 °C. As soon as the black selenium powder was fully consumed and a transparent solution with light yellow color was obtained, ethyl 2-bromoacetate (88.2 g, 528 mmol) was added dropwise and the solution was gradually warmed to room temperature overnight. The reaction was then quenched by addition of saturated aqueous ammonium chloride solution and extracted with diethyl ether. The combined extracts were washed with brine, dried over anhydrous MgSO₄, and then filtered. The solvent was removed by rotary evaporation to yield a brown oil, which was distilled under vacuum. The fraction collected at 90 °C under 0.9 torr as a light yellow oil was identified as the desired product (106.3 g, 89%). The spectroscopic data were consistent with literature.¹

Synthesis of ethyl 2-(2-formylthiophen-3-ylselanyl)acetate (b). To a stirred solution of ethyl 2-(thiophen-3-ylselanyl)acetate (93.4 g, 375 mmol) and *N*-methylformanilide (66.0 g, 488 mmol) in dry 1,2-dichloroethane (600 mL) was dropwise added POCl₃ (69.0 g, 459 mmol) at 0 °C over 30 minutes. The mixture was then refluxed overnight, cooled to room temperature and quenched by addition of saturated aqueous sodium acetate solution and extracted with CH₂Cl₂. The combined extracts were washed with brine, dried over anhydrous MgSO₄, and then filtered. The solvent was removed by rotary evaporation to yield a brown oil, which was then purified by column chromatography on silica gel with hexanes/CH₂Cl₂ (v/v = 1:2) as eluent to afford the desired product (88.4 g, 84%). The spectroscopic data were consistent with literature.¹

*Synthesis of ethyl selenopheno[3,2-*b*]thiophene-5-carboxylate (c).* To a stirred solution of ethyl 2-(2-formylthiophen-3-ylselanyl)acetate (83.1 g, 300 mmol) in DMF (400 mL) was added K₂CO₃ (124.4, 900 mmol) in small portions. The mixture was stirred overnight under room temperature and quenched by addition of saturated aqueous ammonium chloride solution and extracted with ethyl acetate. The combined extracts were washed with brine, dried over anhydrous MgSO₄, and then filtered. The solvent was removed by rotary evaporation to yield a brown oil, which was then purified by

flash column chromatography on silica gel with 2 vol% ethyl acetate in hexanes as eluent to afford the desired product (70.8 g, 91%). The spectroscopic data were consistent with literature.¹

*Synthesis of selenopheno[3,2-*b*]thiophene-5-carboxylic acid (**1**).* To a stirred solution of ethyl selenopheno[3,2-*b*]thiophene-5-carboxylate (51.8 g, 200 mmol) in a THF (400 mL) was added 1 M aqueous LiOH solution (400 mL). The mixture was refluxed overnight, and then cooled to room temperature. The organic volatiles were removed by rotary evaporation, and the residue was added 35% HCl slowly until reaching a pH of 1. The pale yellow precipitate was collected by filtration, washed with water and the air-dried. The crude product was further purified by refluxing in hot hexanes (400 mL) and filtered to give a white solid as the desired product (42.5 g, 92%). The spectroscopic data were consistent with literature.¹

UV-Vis Measurement

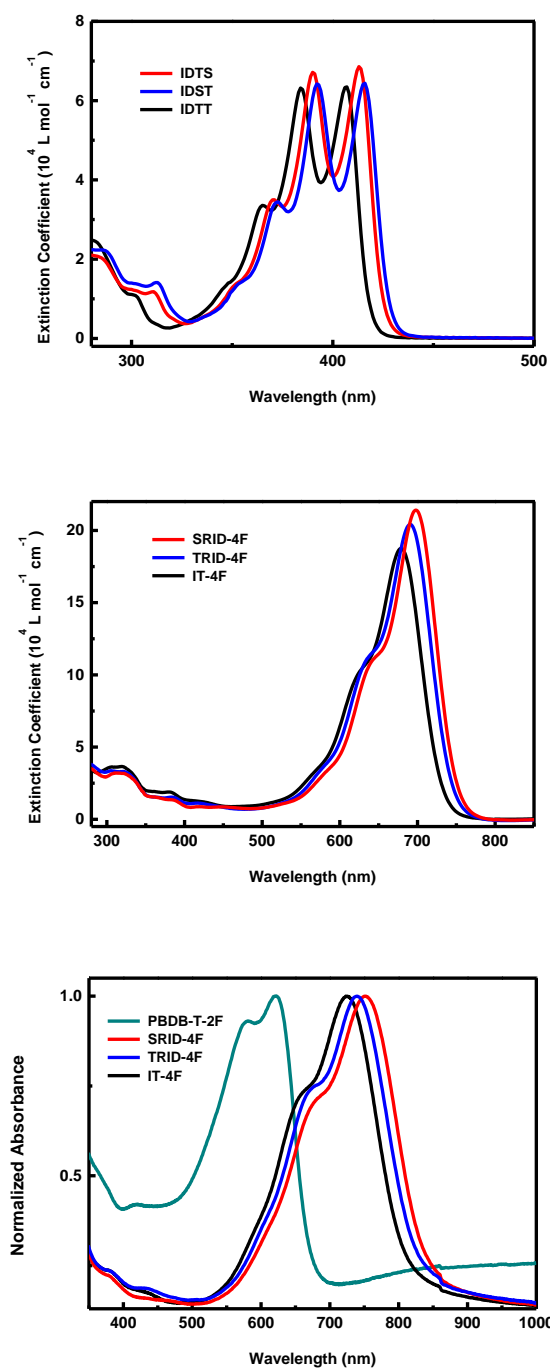


Figure S1 UV-Vis spectra of (a) **IDTS**, **IDST**, and **IDTT** in CH_2Cl_2 ($4 \times 10^{-6} \text{ M}$), (b) **SRID-4F**, **TRID-4F** and **IT-4F** in CH_2Cl_2 ($1 \times 10^{-6} \text{ M}$) and (c) thin film of **SRID-4F**, **TRID-4F** and **IT-4F**.

Electrochemical Measurement

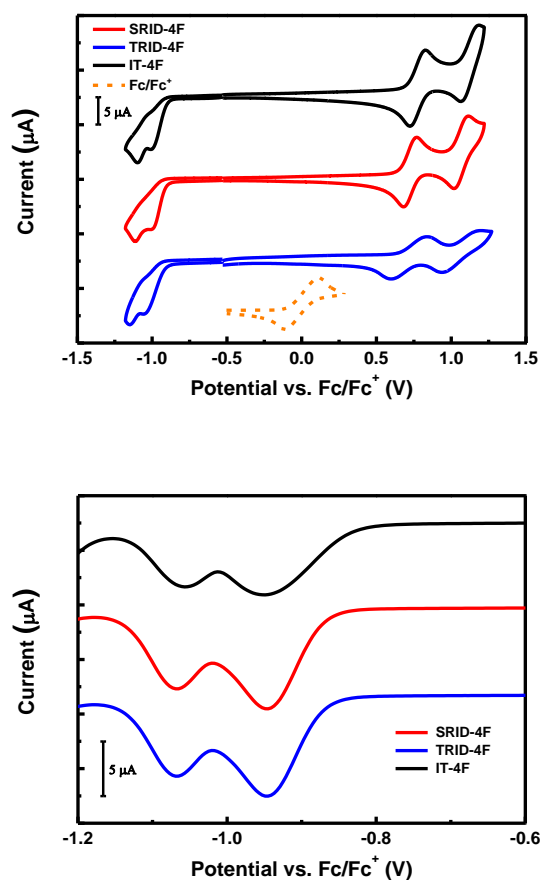


Figure S2 (a) Cyclic voltammogram of **SRID-4F**, **TRID-4F** and **IT-4F**. (b) Differential pulse voltammogram of **SRID-4F**, **TRID-4F** and **IT-4F** in the cathodic potential regime.

Table S1 Summary of UV-Vis and electrochemistry characteristics of NFAs.

	$\lambda_{\text{max, soln}}^a$ (nm)	ϵ^a (10 ⁴ L mol ⁻¹ cm ⁻¹)	$\lambda_{\text{max, film}}^b$ (nm)	λ_{edge}^c (nm)	$E_{\text{g, film}}^d$ (eV)	HOMO ^e (eV)	LUMO ^e (eV)	LUMO ^f (eV)	$E_{\text{g, CV}}^g$ (eV)
SRID-4F	698	21.4	752	862	1.44	-5.52	-3.90	-3.86	1.62
TRID-4F	691	20.4	740	836	1.48	-5.52	-3.90	-3.86	1.62
IT-4F	679	18.8	723	820	1.51	-5.57	-3.89	-3.85	1.68

^a Measured in CH₂Cl₂ solution (1×10⁻⁶ M). ^b Spin-cast thin film. ^c Optical band-gap estimated from thin-film absorption. ^d Calculated from the absorption edge of thin-film spectra. ^e Cyclic voltammetry (CV) was measured in CH₂Cl₂ solution with 0.1 M NBu₄PF₆ as supporting electrolyte. ^f Differential pulse voltammetry (DPV) was measured in CH₂Cl₂ solution with 0.1 M NBu₄PF₆ as supporting electrolyte. Sample concentration was 0.01 M for both CV and DPV measurements. All potentials were recorded using Fc/Fc⁺ as an external reference, which was referenced at -4.80 eV below vacuum level. ^g Electrochemical band-gap estimated from the redox half potentials of CV measurement.

Photovoltaic Device Characteristics

Table S2 Device optimization parameters for PBDB-T-2F:SRID-4F/TRID-4F.

	D:A raio	Processing condition	V_{oc} (V)	J_{sc} (mA/cm ²)	FF	PCE (%)
PBDB-T-2F: SRID-4F	2:1	CB	0.863	19.15	0.723	11.95
	1:1.5	CB	0.872	18.81	0.746	12.24
	1:1.5	CB+0.25% DIO	0.823	20.42	0.749	12.58
	1:1.5	CB+0.25% DIO Annealed at 100 °C	0.844	20.25	0.737	12.58
	1:1	CB+0.25% DIO Annealed at 100 °C	0.846	20.51	0.752	13.05
	1:1	CB+0.25% DIO Annealed at 100 °C Thicker film ~ 150 nm	0.823	8.83	0.586	8.83
PBDB-T-2F: TRID-4F	2:1	CB	0.880	18.11	0.706	11.24
	1:1.5	CB	0.891	17.59	0.734	11.50
	1:1.5	CB+0.25% DIO	0.867	18.04	0.746	11.68
	1:1.5	CB+0.25% DIO Annealed at 100 °C	0.888	18.42	0.747	12.33
	1:1	CB+0.25% DIO Annealed at 100 °C	0.890	17.25	0.750	11.52
	1:1	CB+0.25% DIO Annealed at 100 °C Thicker film ~ 150 nm	0.869	18.59	0.742	11.98
	1:1	CB+0.25% DIO Annealed at 100 °C Thicker film ~ 200 nm	0.871	18.62	0.669	10.85

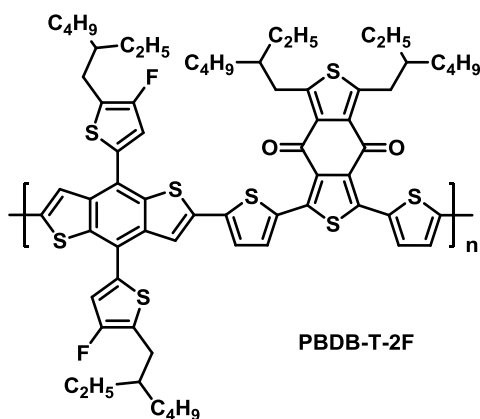


Figure S3 Chemical structure of PBDB-T-2F.

SCLC Characteristics

Space charge-limited currents (SCLC) model was used to evaluate charge carrier mobilities, which were determined by fitting the dark current according to the following equation:

$$J(V) = \frac{9V^2}{8L^3} \varepsilon_0 \varepsilon_r \mu_0$$

Where J is the dark current density (mA cm^{-2}), μ is the zero-field mobility ($\text{cm}^2 \text{V}^{-1} \text{s}^{-1}$), ε_0 is the permittivity of free space, ε_r is the relative permittivity of the material, V is the effective voltage ($V = V_{\text{Applied}} - V_{\text{Built-in}} - V_{\text{series resistance}}$), and L is the thickness of the active layer.

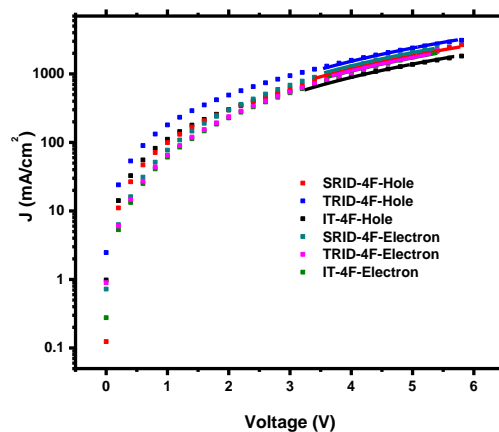


Figure S4 SCLC characteristics of blended films of PBDB-T-2F:SRID-4F/TRID-4F/IT-4F. The solid lines are the fitting curves.

GIWAXS Characteristics

Grazing-incidence wide-angle x-ray scattering (GIWAXS) was carried out at beamline 7.3.3 Lawrence Berkeley National Lab (LBNL). The sample was put inside a helium chamber, and Pilatus 2M detector was used to collect the signal. GIWAXS raw data were analyzed using Nika software package and peak information was assessed by Gaussian fitting. RSoXS was performed at beamline 11.0.1.2 Lawrence Berkeley National Lab. Thin films was flowed and transferred onto Si_3N_4 substrate and experiment was done in transition mode.

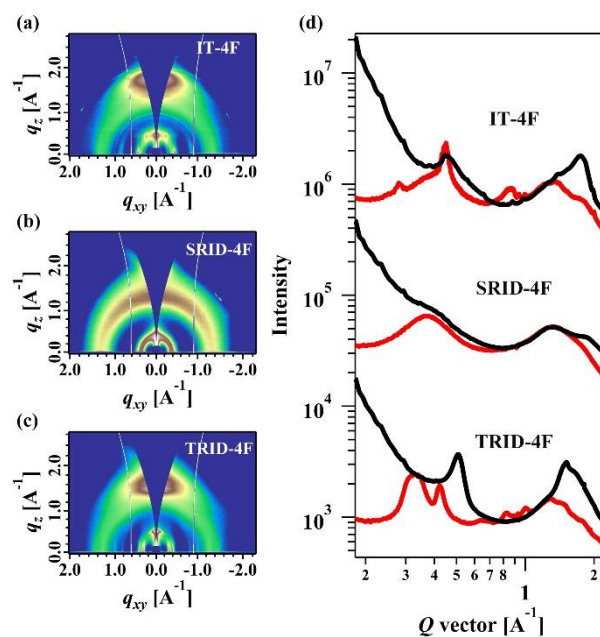


Figure S5 The 2D GIWAXS profile of neat films of (a) **IT-4F**, (b) **SRID-4F**, and (c) **TRID-4F**. (d) In-plane (red line) and out-of-plane (black line) line-cut profile of GIWAXS patterns.

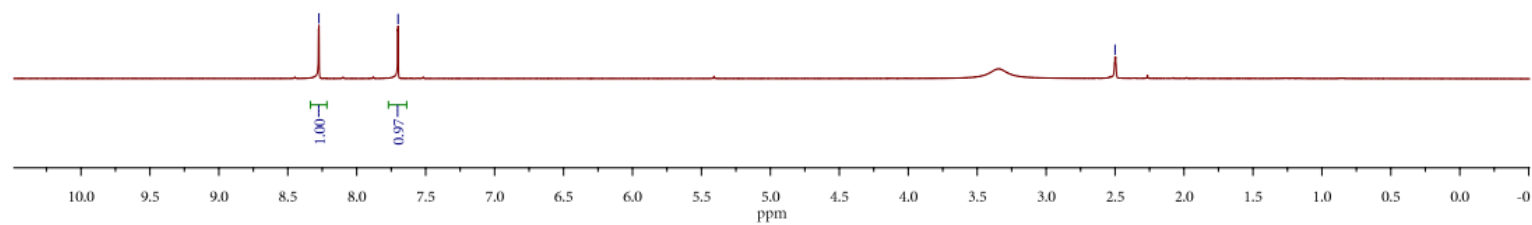
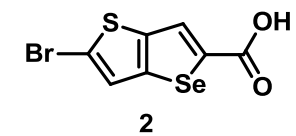
Table S3 Summary of GIWAXS characteristics of NFAs, PBDB-T-2F and blends.

Neat Film	Peak	Position (Å ⁻¹)	FWHM (Å ⁻¹)	<i>d</i> -spacing (Å)	CCL (Å)	
PBDB-T-2F	100	0.29	0.079	21.66	71.58	
	010	1.70	0.470	3.69	12.03	
IT-4F	100	0.38	0.096	16.53	58.90	
	010	1.75	0.294	3.59	19.23	
SRID-4F	100	0.37	0.201	16.98	28.13	
	010	1.84	0.602	3.41	9.40	
TRID-4F	100	0.33	0.041	19.03	137.92	
	010	1.61	0.620	3.90	9.12	
Blend	Peak	Position (Å ⁻¹)	FWHM (Å ⁻¹)	Area	<i>d</i> -spacing (Å)	CCL (Å)
PBDB-T-2F:IT-4F	100	0.292	0.0378	45.26	21.50	149.72
	010	3.61	0.3681	184.14	3.61	15.36
PBDB-T-2F:SRID-4F	100	0.293	0.0319	48.92	21.43	177.08
	010	3.56	0.3207	212.25	3.56	17.63
PBDB-T-2F:TRID-4F	100	0.290	0.0354	41.28	21.63	159.84
	010	3.64	0.3752	174.48	3.64	15.07

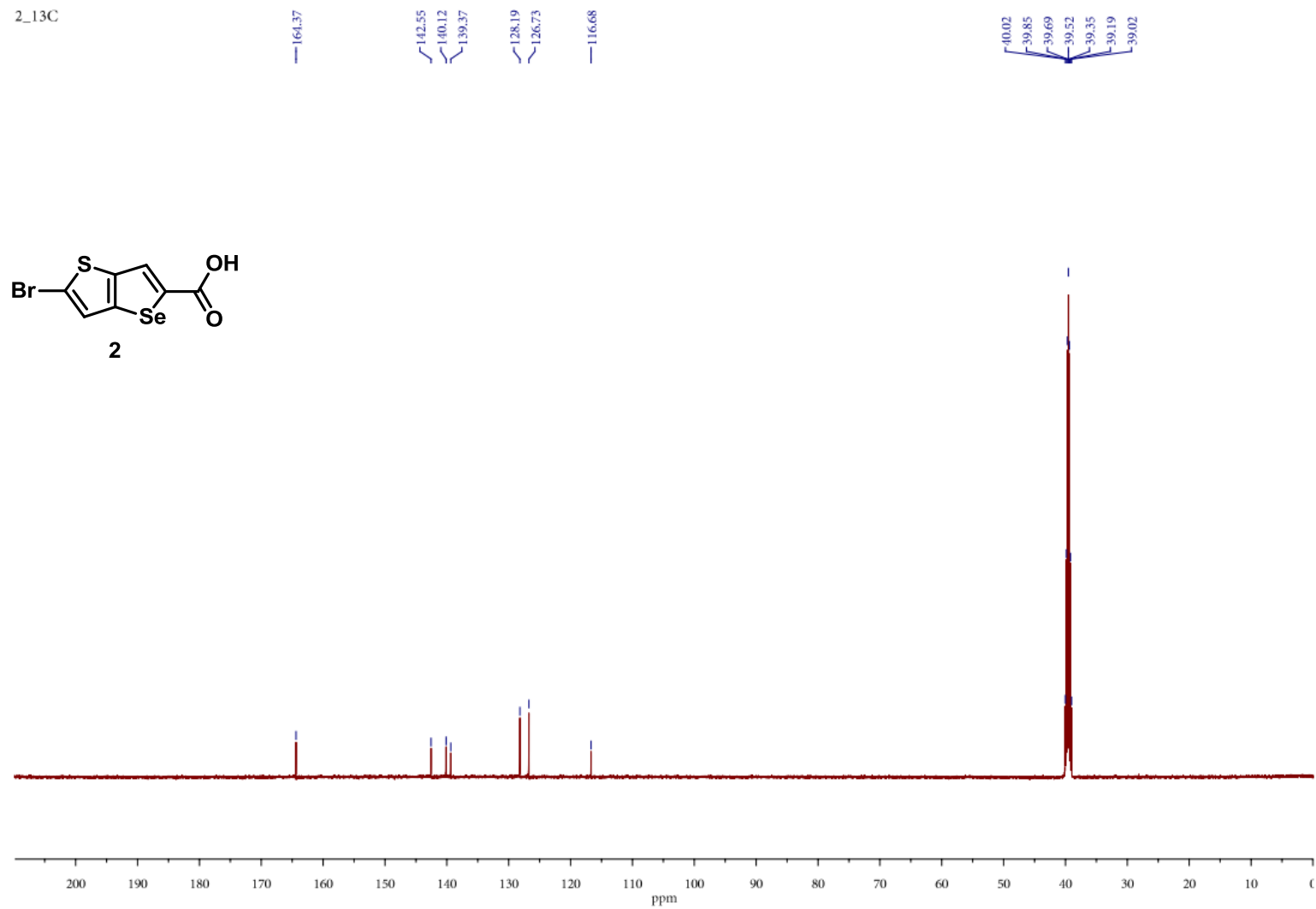
Reference

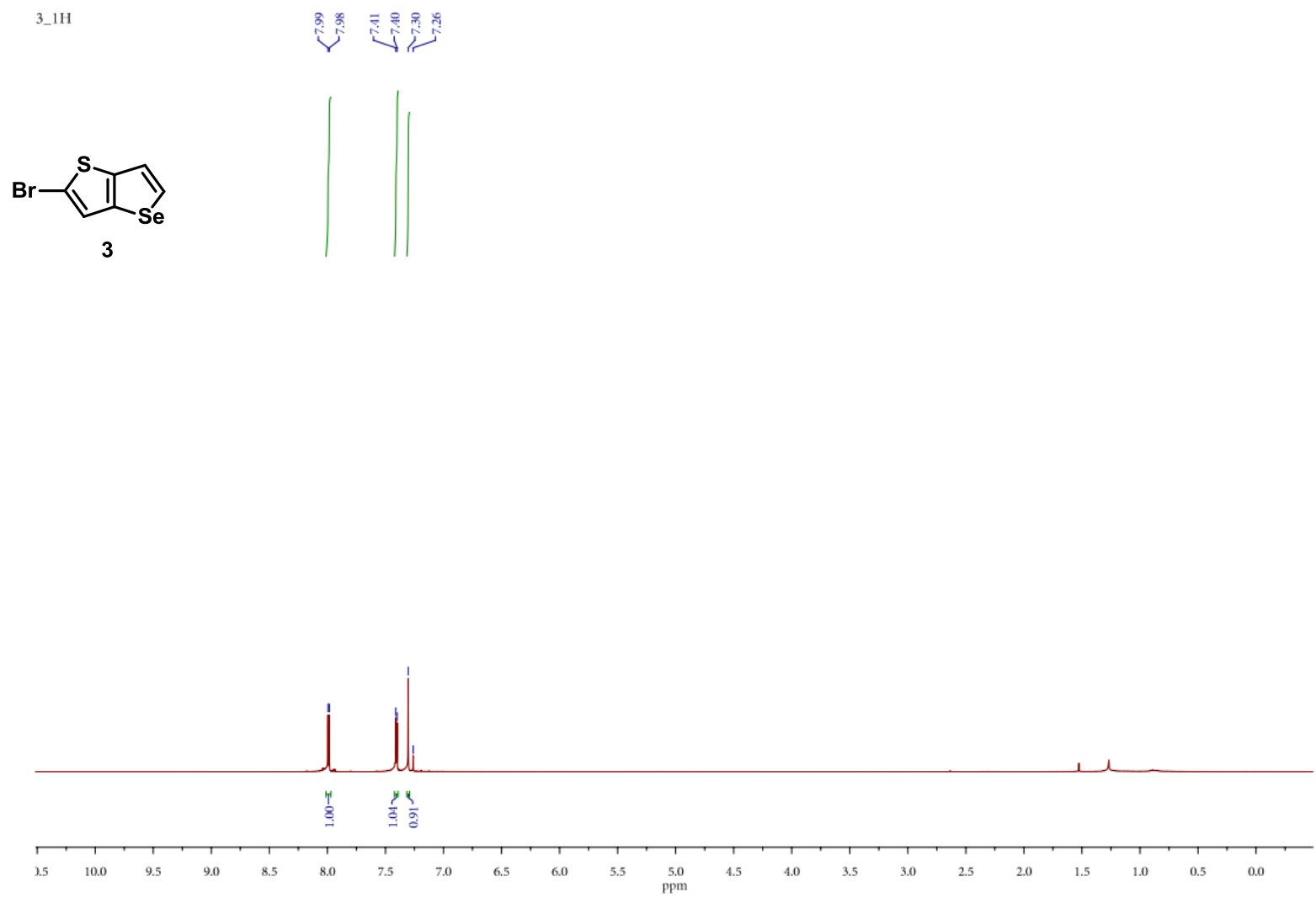
1. Mishra, S. P.; Javier, A. E.; Zhang, R.; Liu, J.; Belot, J. A.; Osaka, I.; McCullough, R. D. Mixed selenium-sulfur fused ring systems as building blocks for novel polymers used in field effect transistors. *J. Mater. Chem.*, **2011**, *21*, 1551-1561.

2_1H

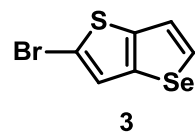


2_13C

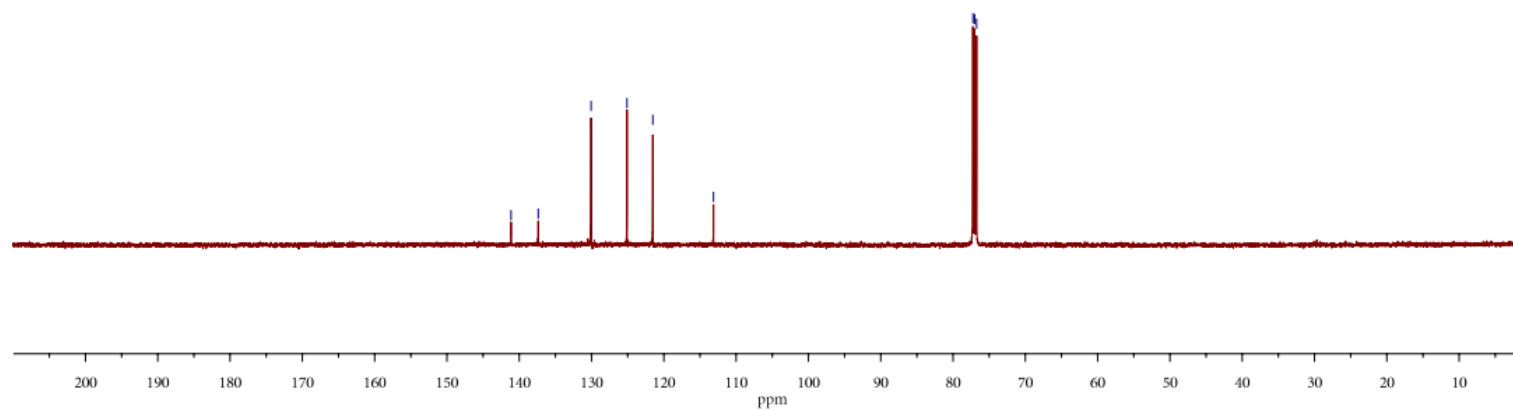




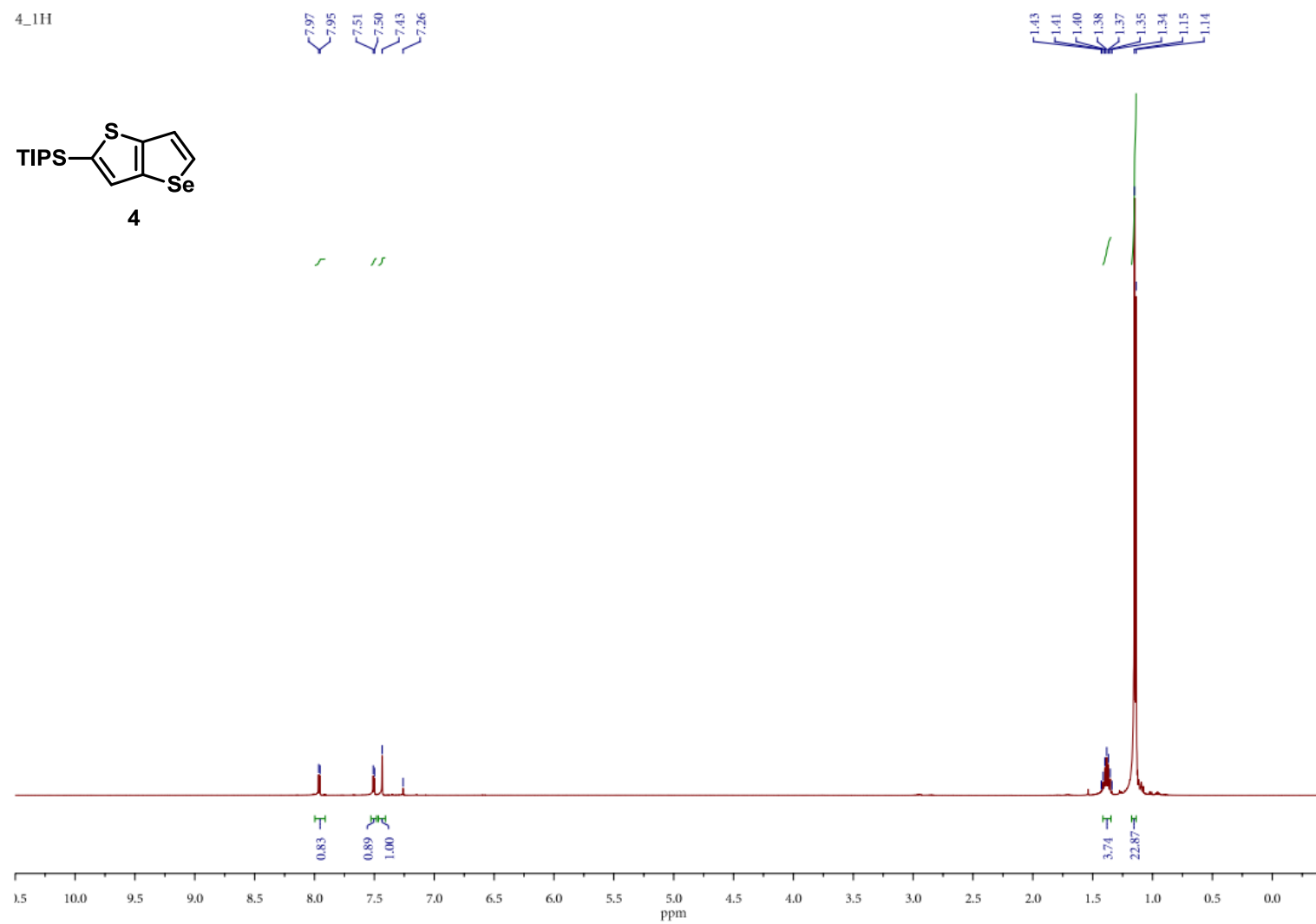
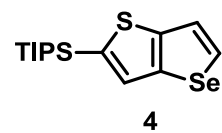
3_13C



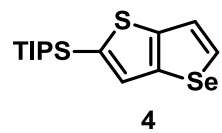
141.13
137.37
130.06
125.10
121.52
113.14
77.25
77.00
76.75



4_1H



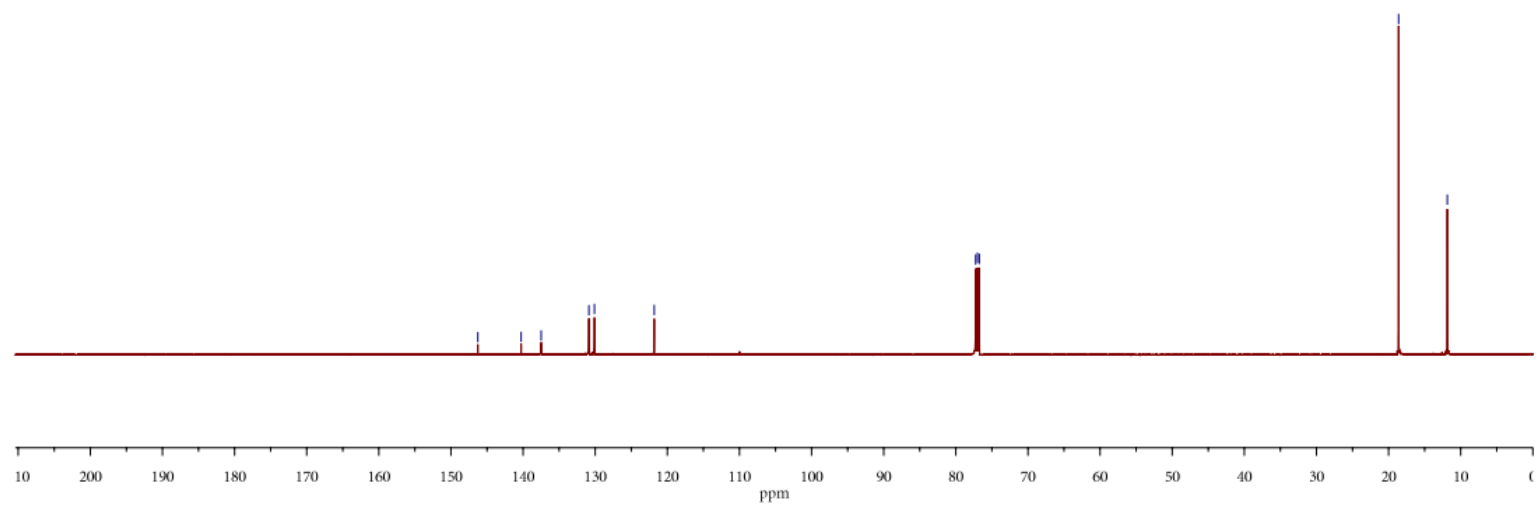
4_13C

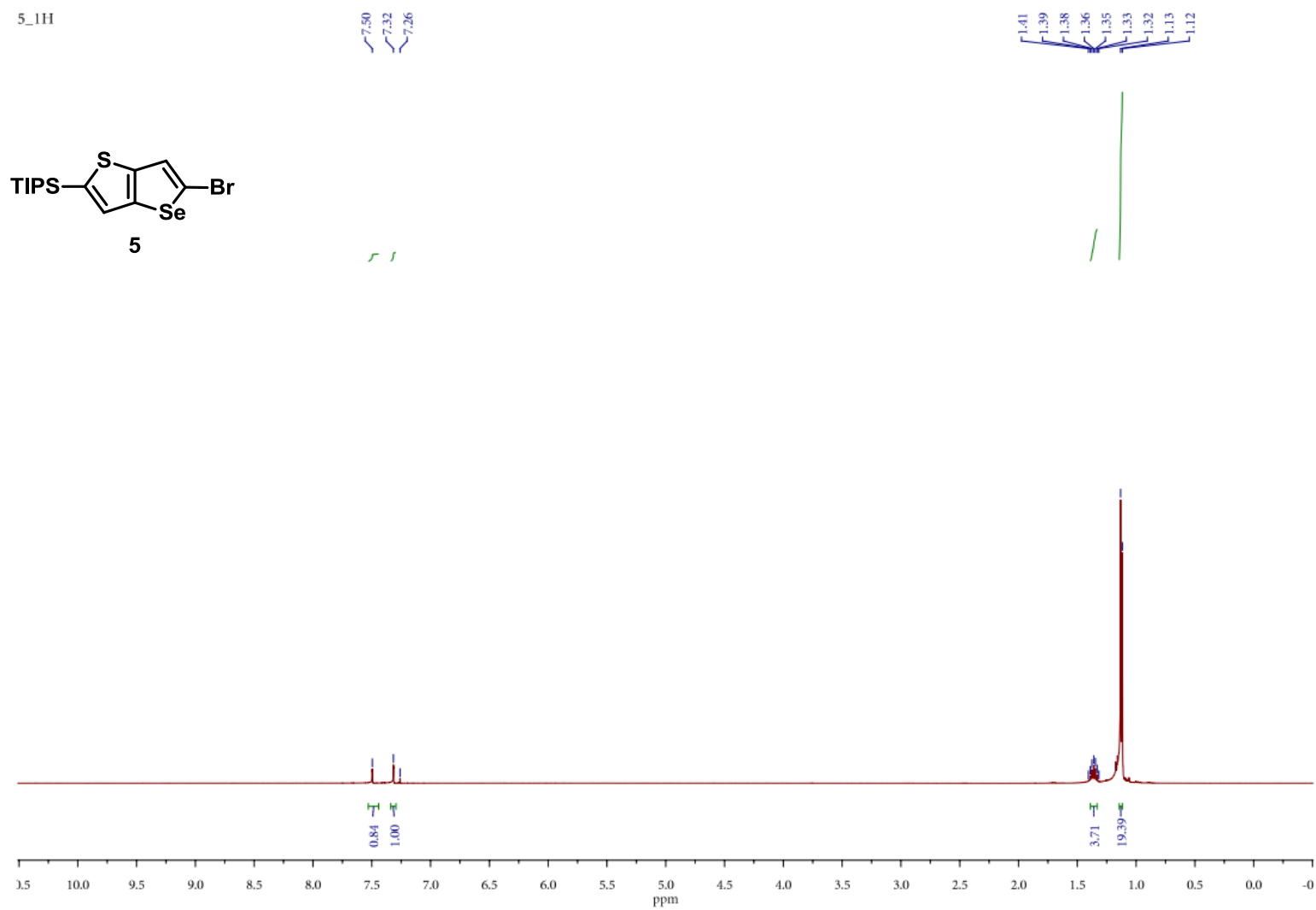


146.27
140.27
137.49
130.88
130.10
121.81

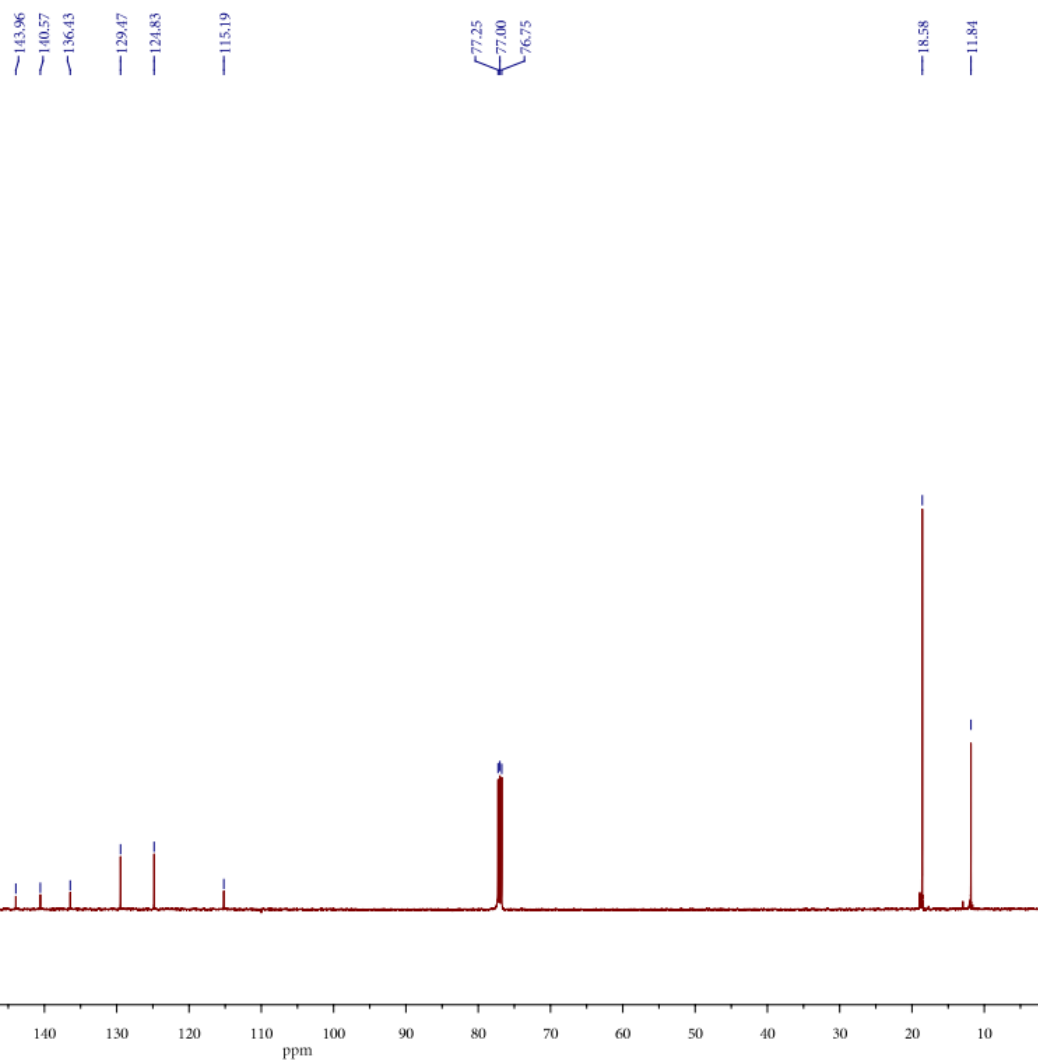
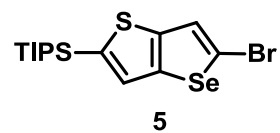
77.25
77.00
76.75

18.61
11.86

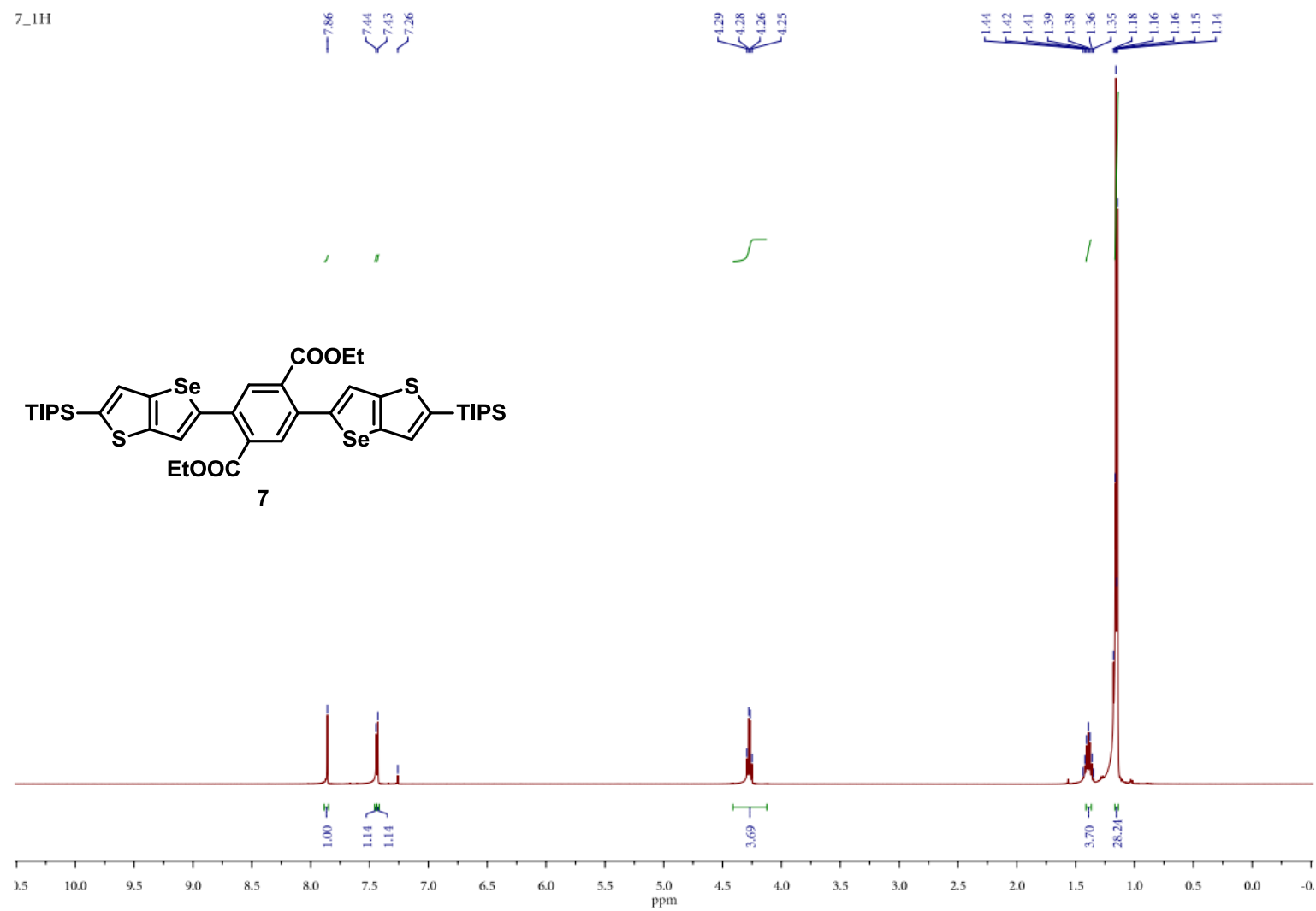




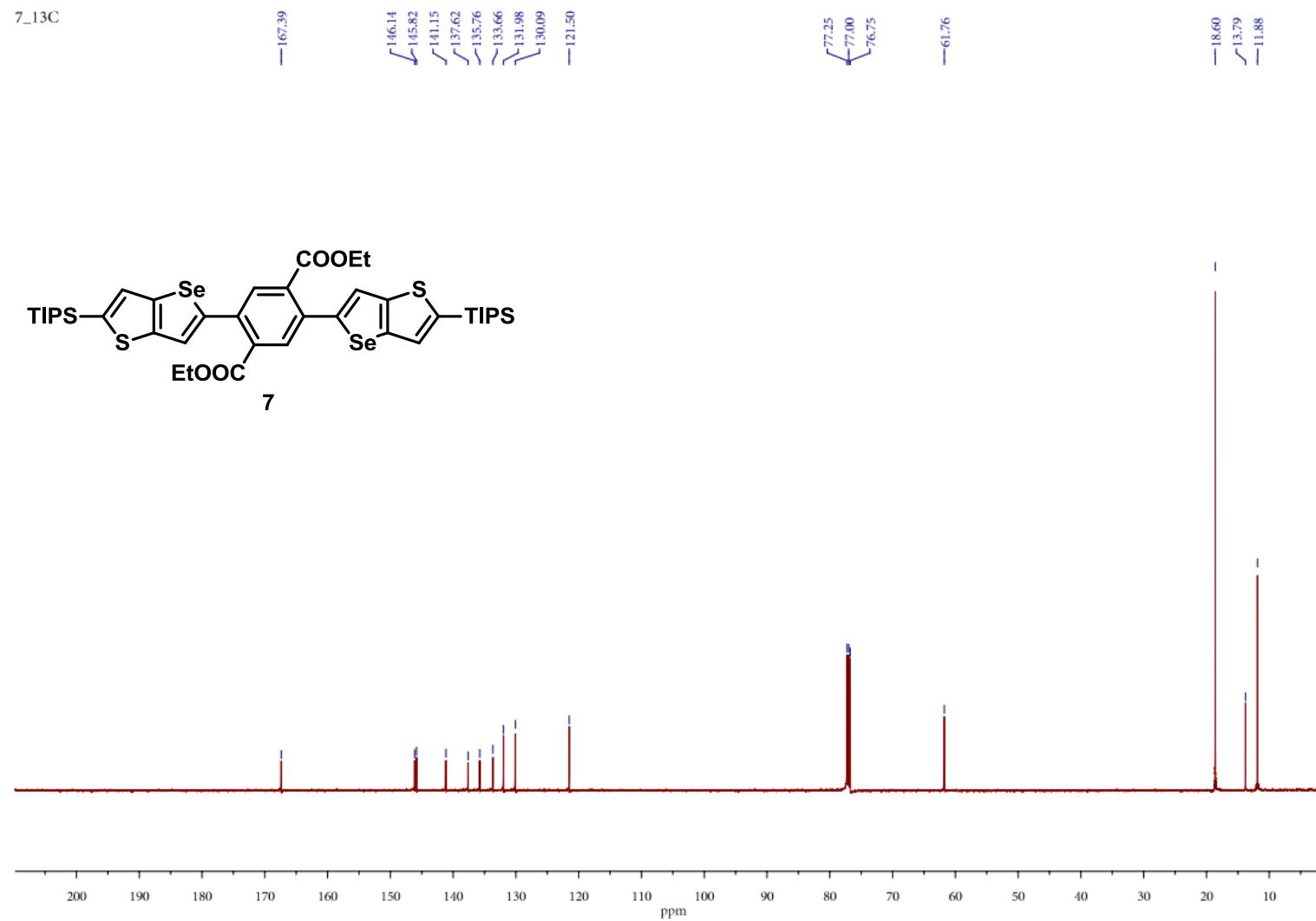
5_13C

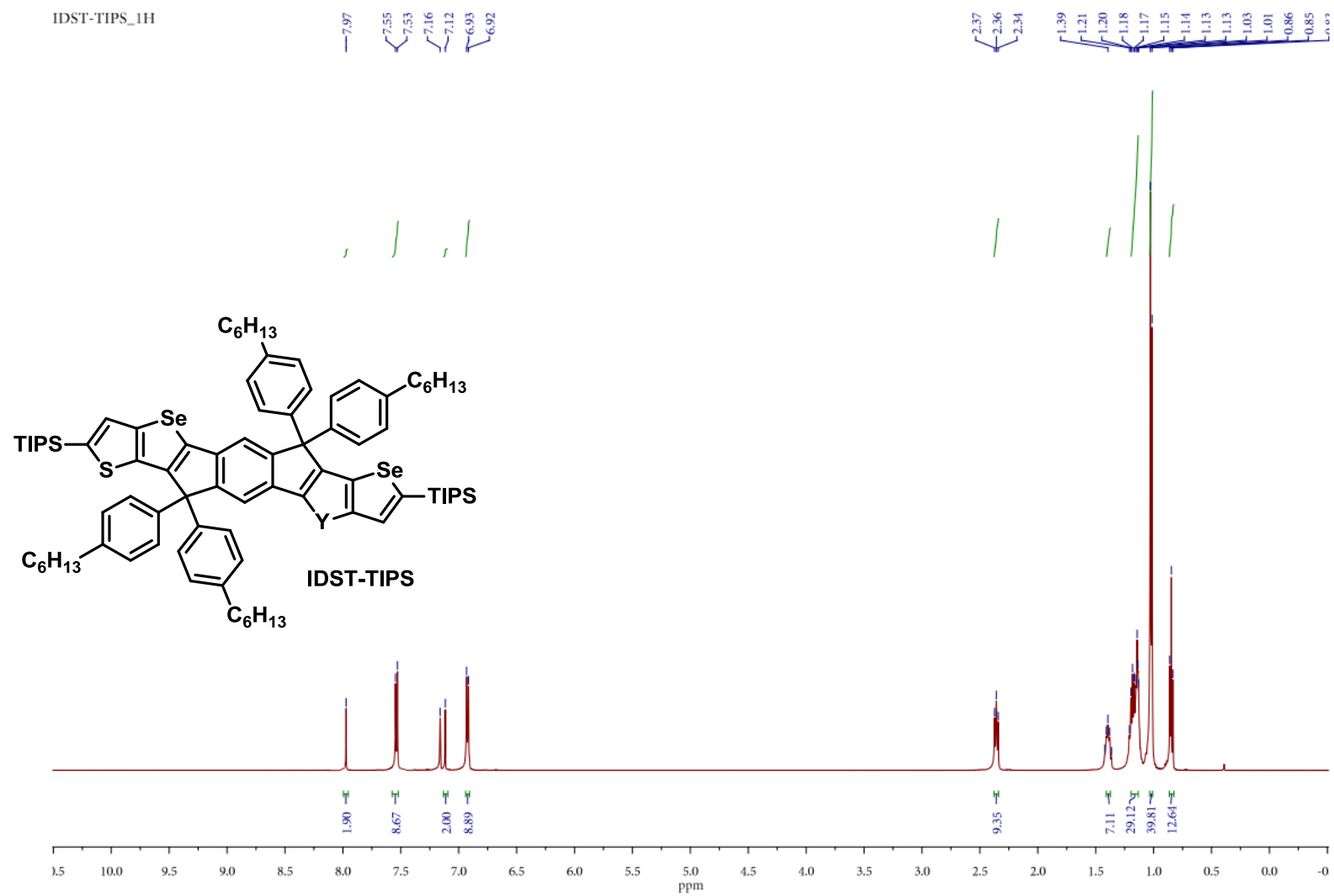


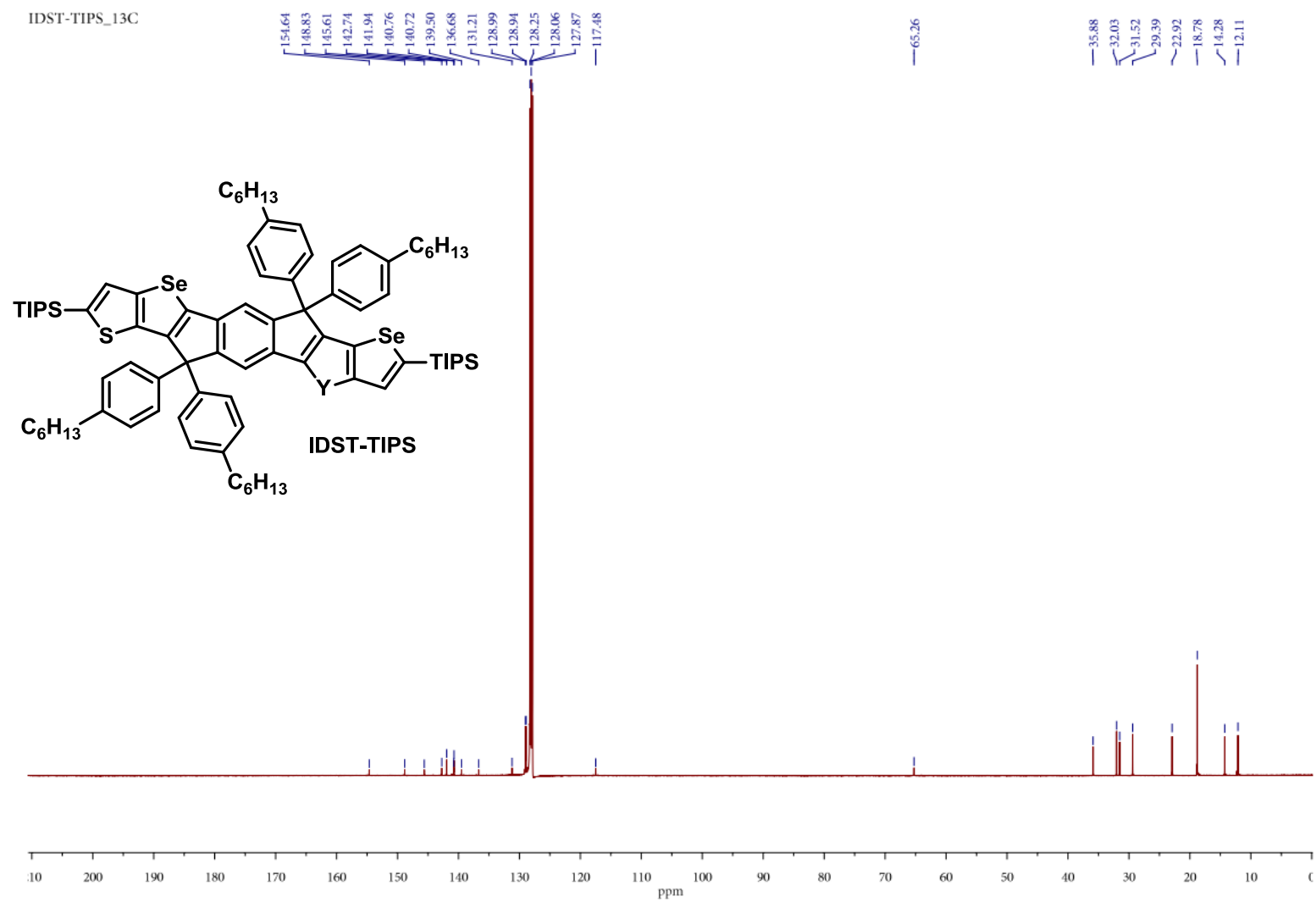
7_1H

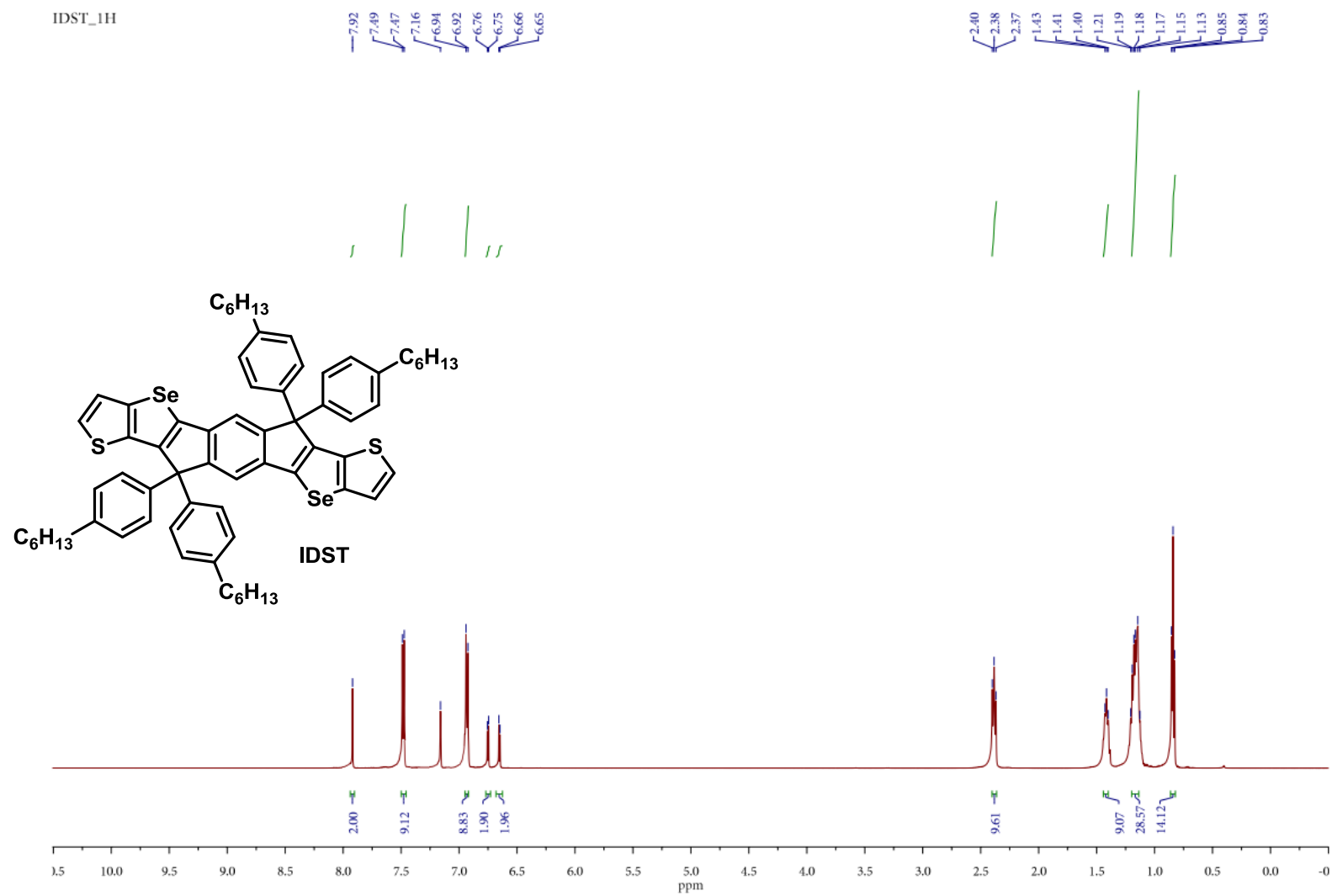


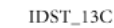
7_13C

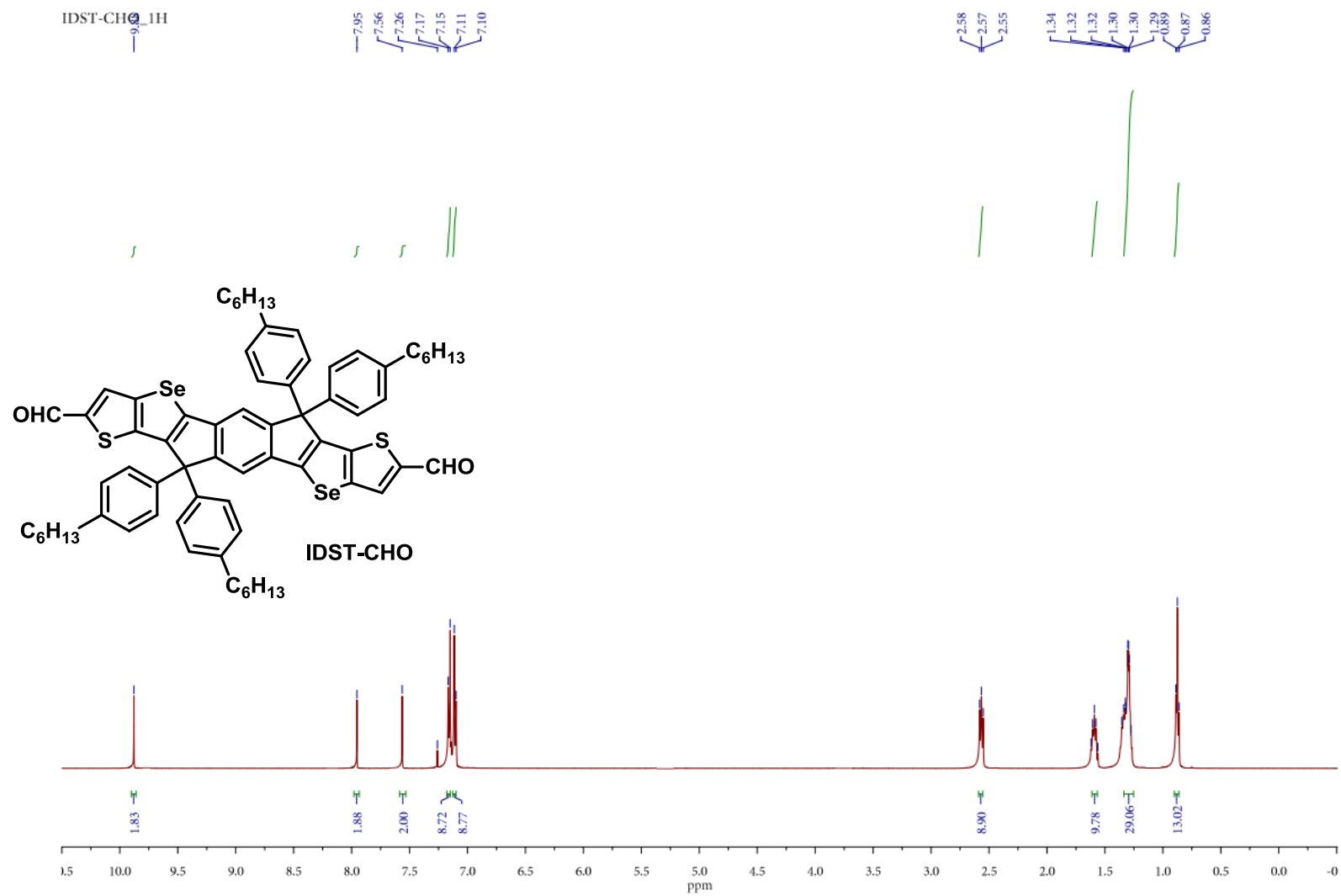


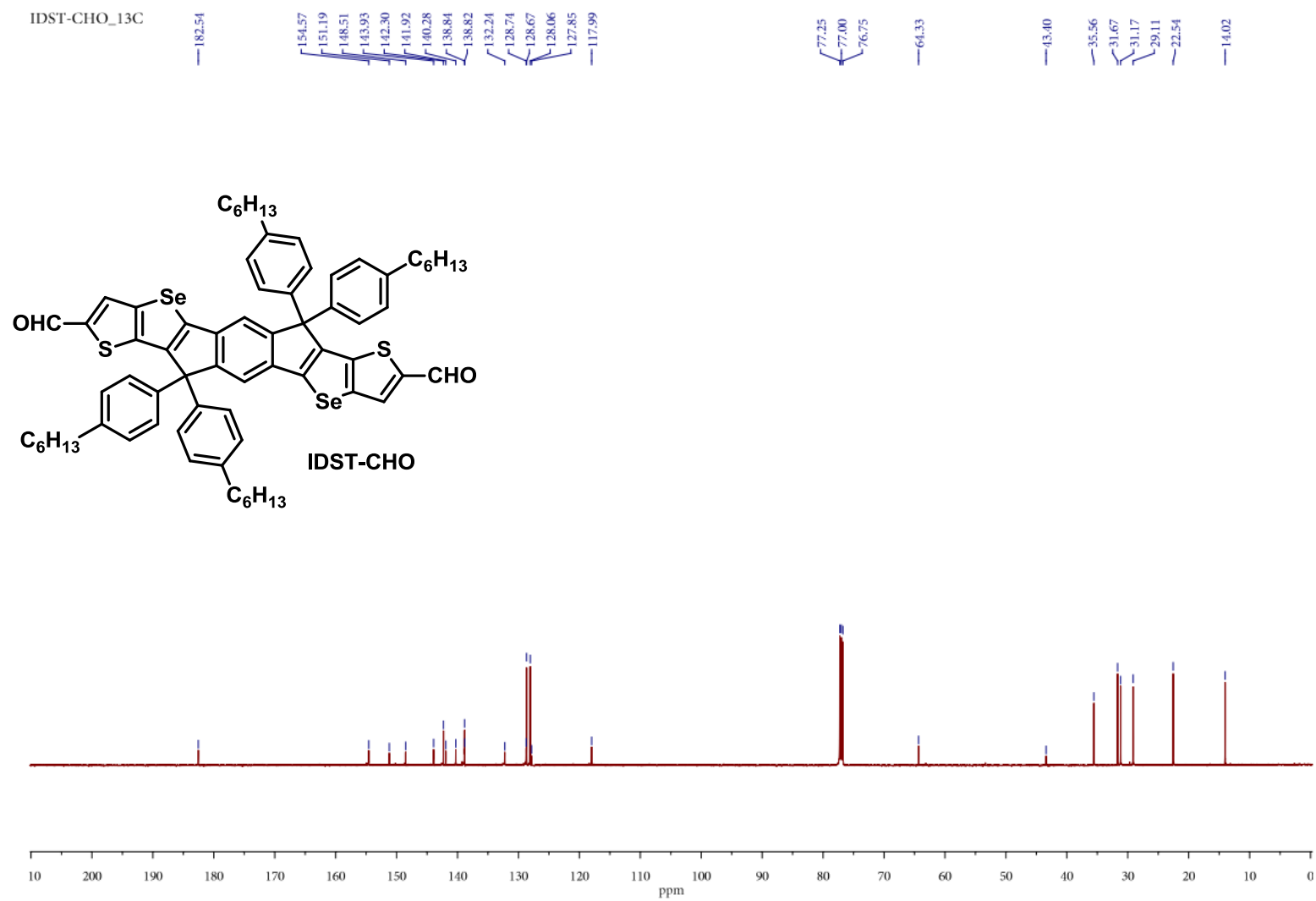


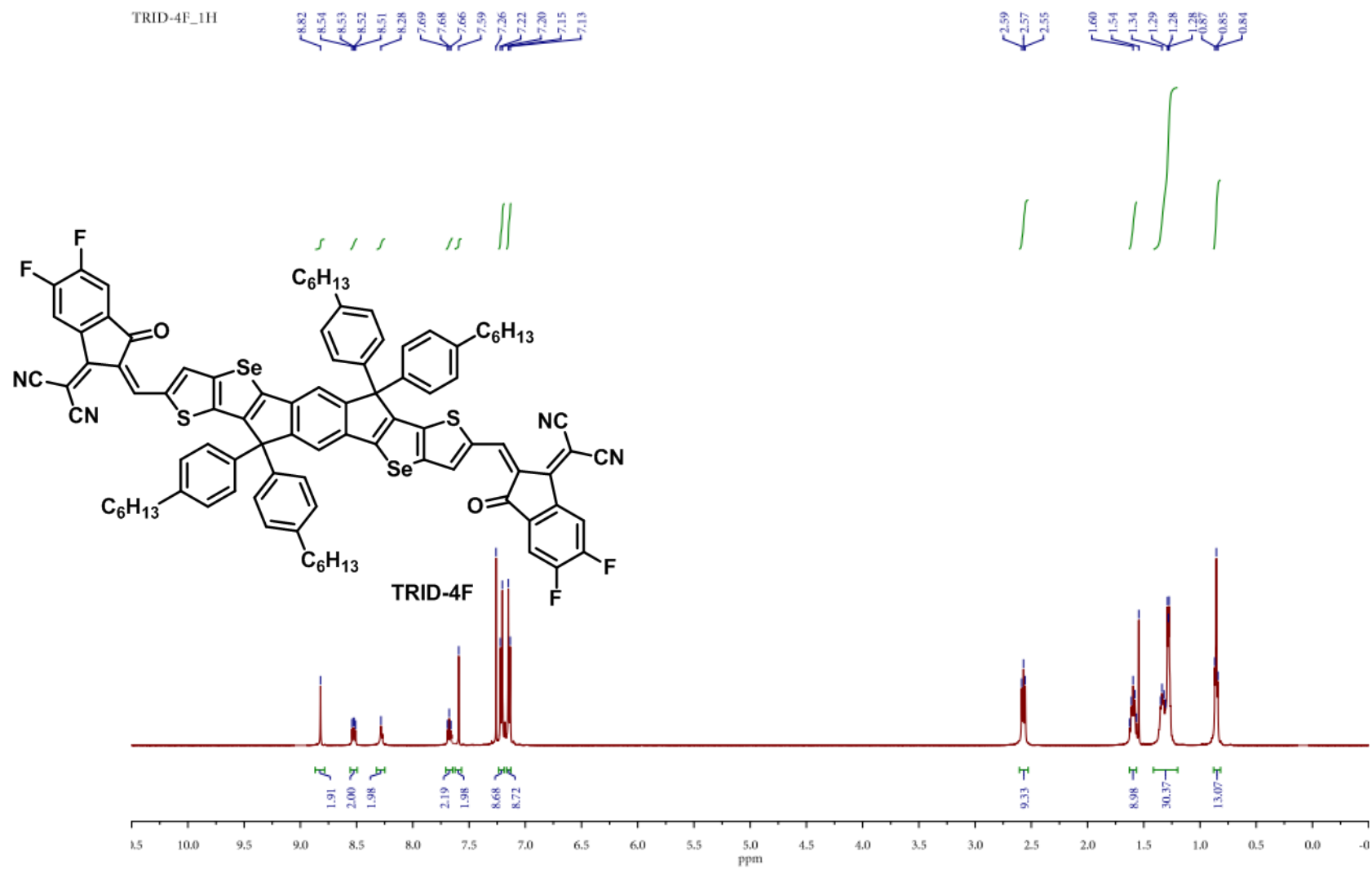


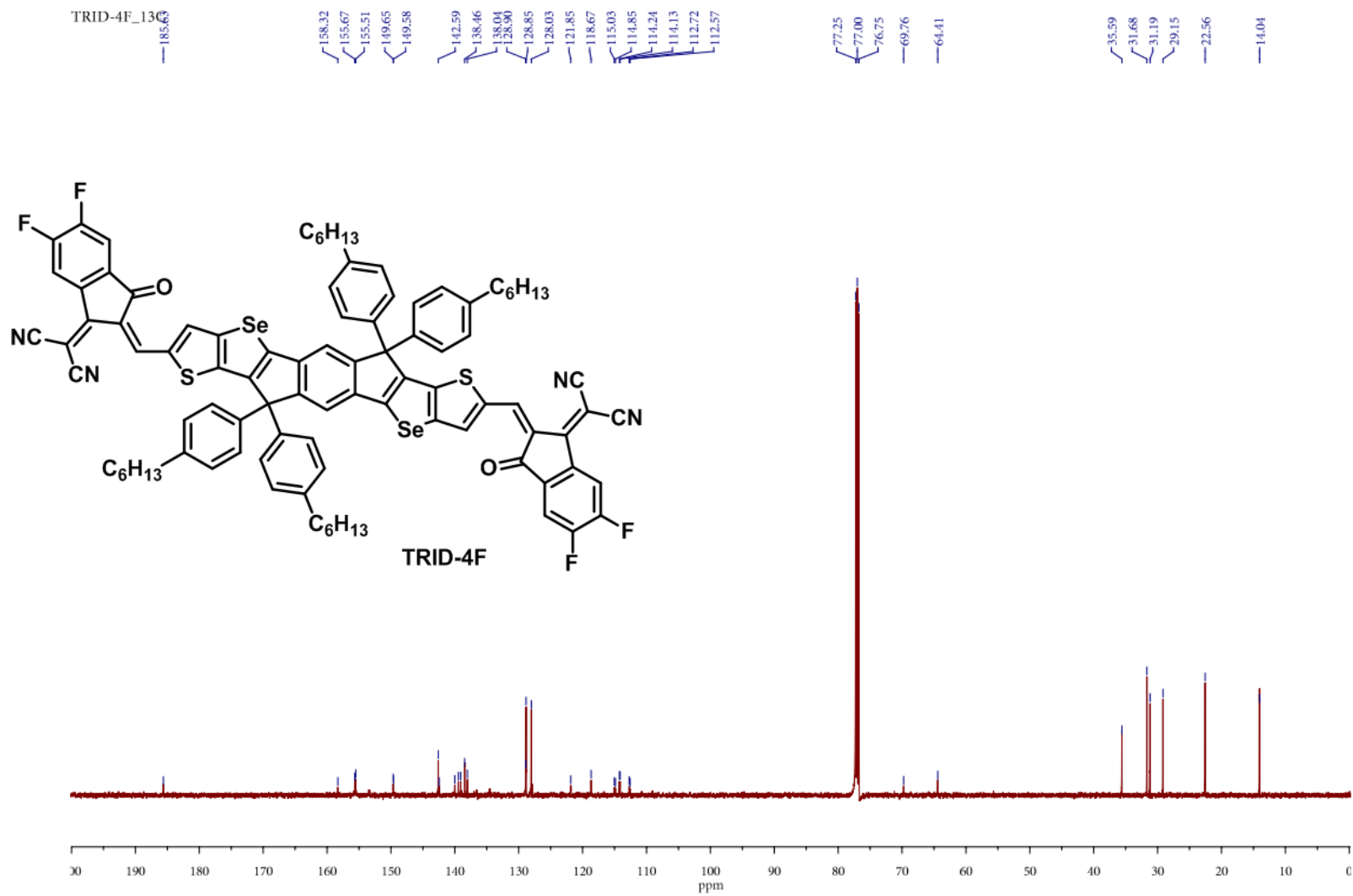




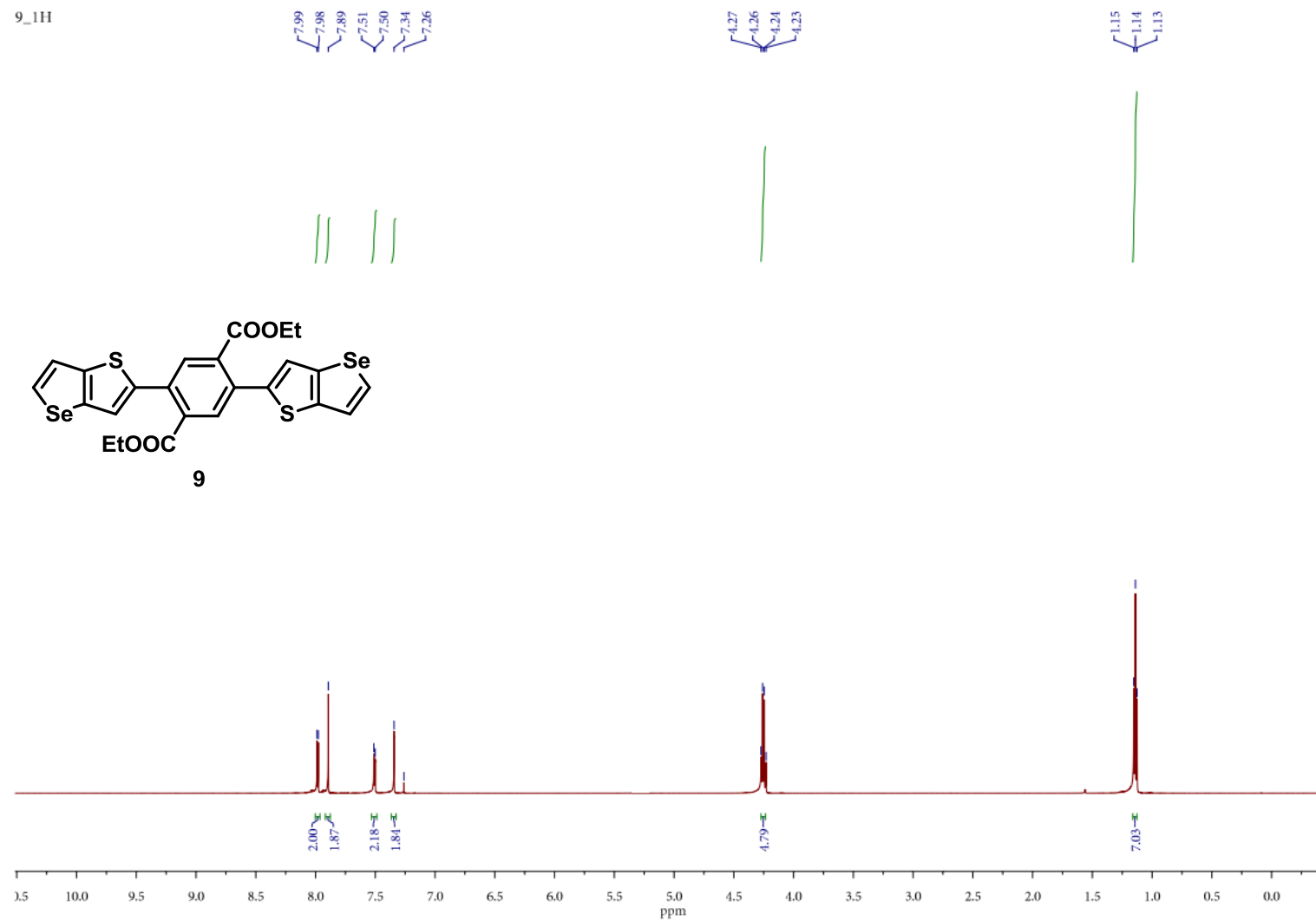








9_1H



9_13C

167.43

141.70

141.58

138.72

134.06

133.58

131.99

130.76

122.44

122.02

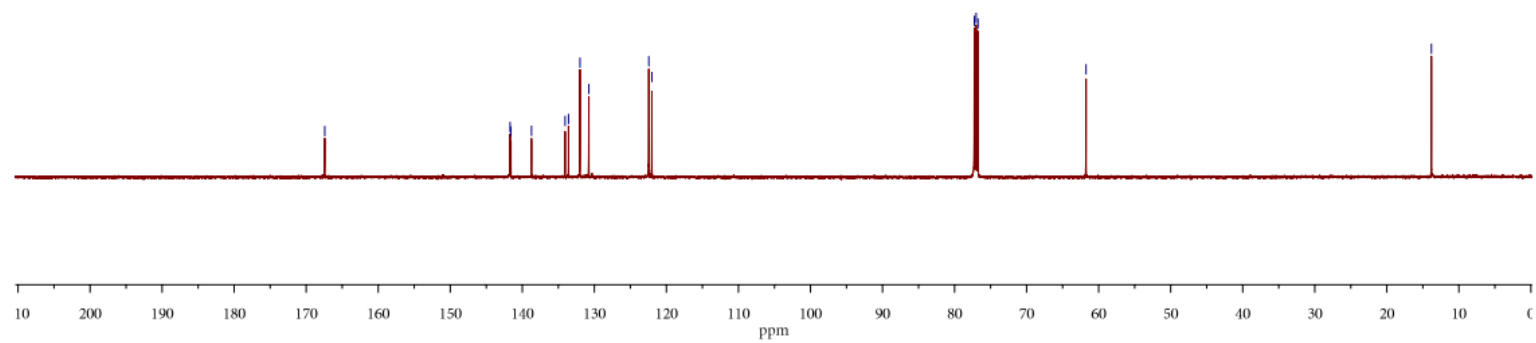
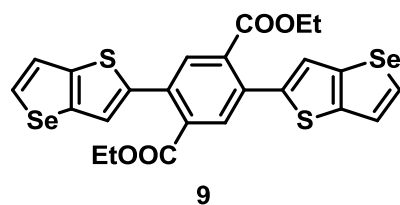
77.25

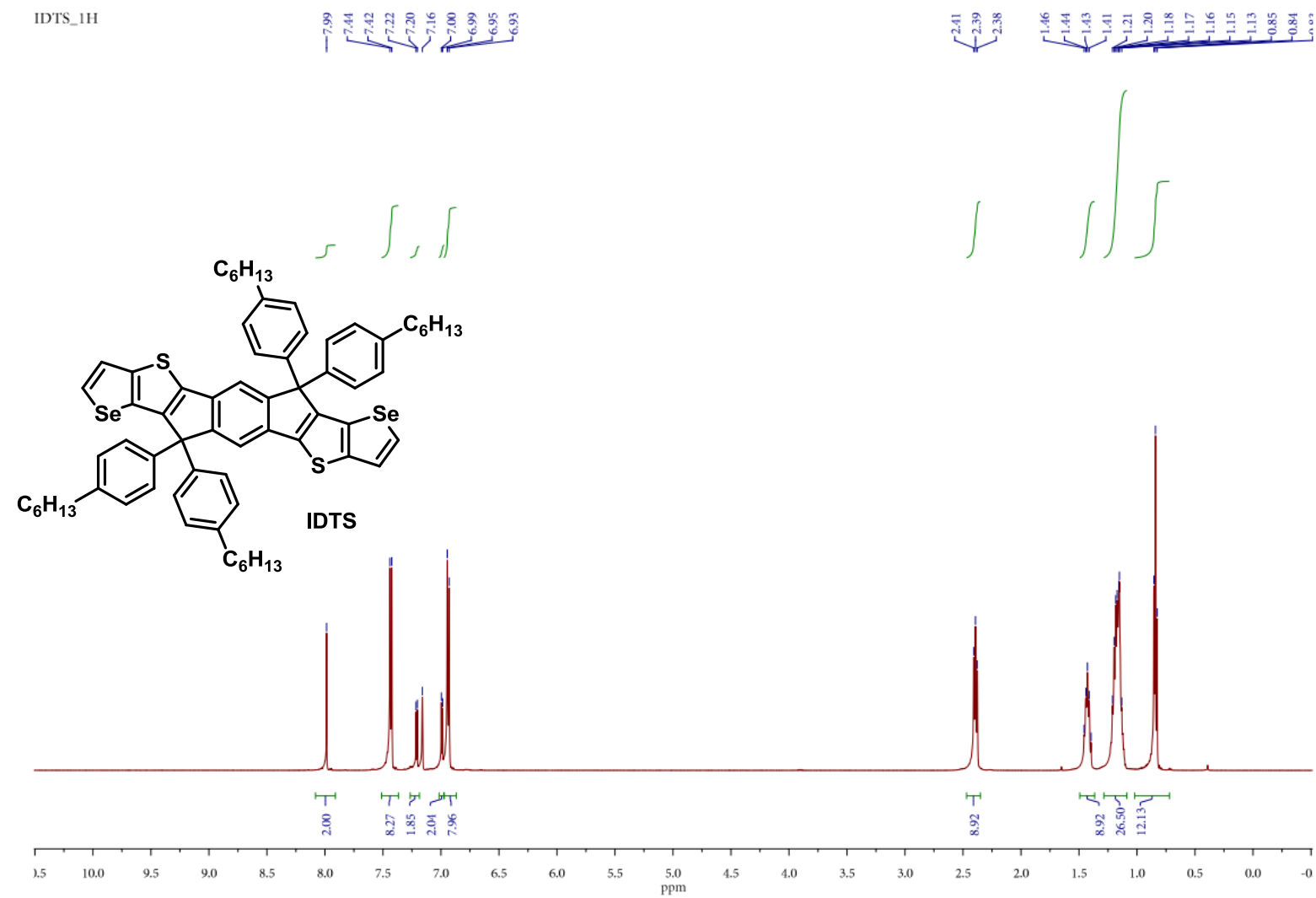
77.00

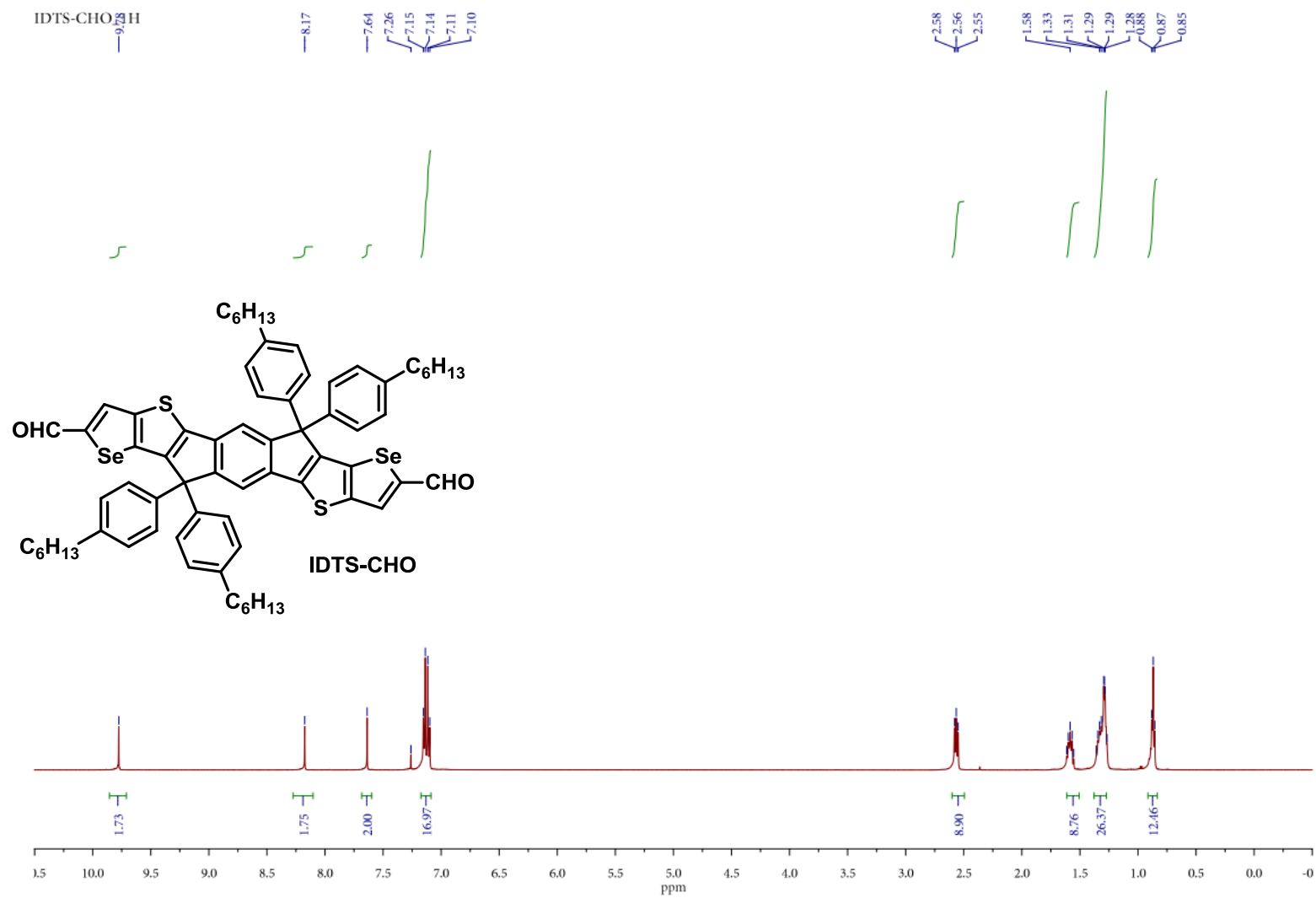
76.75

61.75

13.81







IDTS-CHO_13C

